

Discovering a change point in a time series of organoid networks via the iso-mirror

Tianyi Chen¹, Youngser Park¹, Ali Saad-Eldin¹, Zachary Lubberts¹, Avanti Athreya¹, Benjamin D. Pedigo¹, Joshua T. Vogelstein¹, Francesca Puppò², Gabriel A. Silva², Alysson R. Muotri², Weiwei Yang³, Christopher M. White³, and Carey E. Priebe¹

¹Johns Hopkins University

²University of California San Diego

³Microsoft Research

Recent advancements have been made in the development of cell-based *in-vitro* neuronal networks, or organoids. In order to better understand the network structure of these organoids, [6] propose a method for inferring effective connectivity networks from multi-electrode array data. In this paper, a novel statistical method called spectral mirror estimation [2] is applied to a time series of inferred effective connectivity organoid networks. This method produces a one-dimensional iso-mirror representation of the dynamics of the time series of the networks. A classical change point algorithm is then applied to this representation, which successfully detects a neuroscientifically significant change point coinciding with the time inhibitory neurons start appearing and the percentage of astrocytes increases dramatically [9]. This finding demonstrates the potential utility of applying the iso-mirror dynamic structure discovery method to inferred effective connectivity time series of organoid networks.

1 Introduction

Detecting structural changes in time series of networks is central to many modern network science applications. However, due to the complexity of temporal network data and the myriad possible aspects for potential structural change, this problem can be daunting. For discovering underlying dynamics in time series of networks, [2] proposes theory and methods for representing temporal network structure with a curve, or ‘mirror,’ in low dimensional Euclidean space, enabling the use of classical change point detection algorithms. In this paper, we estimate the mirror for a time series of brain organoid connectivity networks and subsequently identify change points. Because the mirror estimation method requires a 1-1 vertex correspondence for the networks across time, we first demonstrate that the putative 1-1 correspondence obtained directly from data collection is sufficiently accurate by comparing it to the vertex correspondence obtained via graph matching [10]. Thence, mirror estimation and manifold learning recovers a 1-dimensional piecewise linear ‘iso-mirror’ representation, with an evident slope change. By using the change point detection algorithm from [3] and break point estimation for piecewise linear models from [4], we identify a change points neuroscientific significance coinciding with development stages.

We organize this paper as follows. In Section 2 we introduce our brain organoids data and the extraction of effective connectivity networks based on extracellular electrophysiology recordings. In Section 3 we define the graph matching problem and present the fast approximate assignment algorithm. In Section 4 we introduce the

mirror estimation method and relevant model assumptions. In Section 5 we apply these methods to the time series of organoid networks and present the graph matching results and the change point detection results. We conclude with a discussion in Section 6.

2 Organoids

The brain organoids we consider are self-organizing structures composed of roughly 2.5 million neural cells. They are generated from human induced pluripotent stem cells (hiPSCs) [5]. After growing for 6 weeks, they are plated in 8 wells of a multi-electrode array (MEA) plate (Axion Biosystem, Atlanta, GA, USA). MEA contains 64 low-impedance (0.04 MU) platinum microelectrodes with 30 mm of diameter spaced by 200 mm. Each well contains two or three organoids. Then, to characterize the functional development of the organoids, extracellular spontaneous electrical activity is recorded weekly using Maestro MEA system and AxIS Software Spontaneous Neural Configuration (Axion Biosystems) with a 0.1-Hz and 5-kHz band-pass filter. Then spikes are detected with an adaptive threshold crossing set to 5.5 times the standard deviation of the estimated noise for each electrode. Five minutes of data were recorded. After processing, the spike-sorted activity of each well across 10 months is obtained by applying a standard protocol based on principal component analysis (PCA) and k-means clustering. To infer the effective connections between neurons – i.e., the adjacency matrices with neurons as vertices across time from the spike activity data – the algorithm proposed in [6] is applied. This algorithm uses a super-selection rule to individuate and discard correlation peaks corresponding to apparent and indirect interactions, and reconstructs the effective connectivity of the network considering the remaining correlation delays. In the end, 40 effective connectivity networks on 124 neurons across 244 days are obtained. This is our time series of organoid networks.

3 Graph Matching

Given a time series of networks G_1, \dots, G_T on the same set of vertices V , a 1-1 vertex correspondence across all the networks facilitates joint spectral embedding, which is a key step in the mirror estimation method we will present in Section 4. Such a vertex correspondence may be available a priori in labeled networks, or it can be inferred from unlabeled networks. This inference problem – the so-called graph matching problem – is to find an alignment of vertices between two graphs such that the corresponding edge differences are minimized. We denote A, B as two $n \times n$ adjacency matrices for two graphs with n vertices each. Then the graph matching problem is to find the permutation matrix P that maximizes the objective function

$$f(A, B; P) = -\|A - P^T B P\|_F^2$$

for $P \in \mathcal{P}$ where $\mathcal{P} = \{P \in \{0, 1\}^{n \times n} : P^T \mathbf{1} = P \mathbf{1} = \mathbf{1}\}$, $\mathbf{1} = (1, 1, \dots, 1)^T$, and $\|\cdot\|$ denotes the Frobenius norm. This formulation is equivalent to maximizing

$$f(A, B; P) = \text{trace}(A P B^T P^T).$$

Because solving this optimization problem is combinatorically difficult, approximation algorithms have been proposed. We use the Fast Approximate Quadratic (FAQ) assignment algorithm [10] to obtain an approximate solution. FAQ iteratively finds a local solution to the relaxed problem – expanding the constraint set to the convex

hull of \mathcal{P} – and then projects the solution back to \mathcal{P} , and has been shown empirically to be competitive with or superior to other state-of-art methods. In Section 5.2 we use FAQ to demonstrate that the given putative 1-1 correspondence for each pair of networks is close to the solution to the corresponding graph matching problem.

4 Discovering underlying dynamics in time series of networks

To discover the underlying dynamics in time series of networks, we use the model and method proposed in [2]. First we introduce the generative joint model for time series of networks. We consider T networks, each containing n vertices, with adjacency matrices A_t , $t \in \{1, 2, \dots, T\}$. In the model, each vertex is associated with a time varying d -dimensional latent vector. These vectors X_t are each one realization from a stochastic process, called the latent position process (LPP) – each X_t is a d -dimensional random variable. For n vertices, we generate n i.i.d. samples from the LPP, which collection then forms the latent position matrices $\{\mathbf{X}_t\}$, where $\mathbf{X}_t \in \mathcal{R}^{n \times d}$ for $t \in \{1, 2, \dots, T\}$. The connection probability between vertex i and vertex j at time t is the inner product of the associated latent vectors at time t . That is $\mathbb{E}(A_t) = \mathbf{X}_t \mathbf{X}_t^T$. Note that each network corresponds to a latent position random variable. Thus we can capture the distance between graphs using the corresponding random variables. We define the distance

$$d_{MV}(X_t, X_{t'}) = \min_{W \in \mathcal{O}^{d \times d}} \|\mathbb{E}[(X_t - WX_{t'})(X_t - WX_{t'})^T]\|_2^{1/2}.$$

We evaluate this distance for every pair of random variables in the LPP and obtain a $T \times T$ distance matrix \mathcal{D} . Then we apply classical multidimensional scaling (MDS) [8] to \mathcal{D} to get a low-dimensional Euclidean representation of underlying network structure, called the *mirror*, $\{\psi(t)\}$. In practice, the LPP is unknown and only network realizations $\{A_t\}$ are observed. For the $n \times n$ symmetrized adjacency matrix A_t , we use adjacency spectral embedding (ASE) [1] to obtain $\hat{\mathbf{X}}_t = U\Sigma^{1/2}$, where the diagonal matrix Σ contains the top d eigenvalues of A_t and U contains the associated eigenvectors. Then we use

$$\hat{d}_{MV}(\hat{\mathbf{X}}_t, \hat{\mathbf{X}}_{t'}) = \min_W \|\hat{\mathbf{X}}_t - \hat{\mathbf{X}}_{t'} W\|_2^{1/2}$$

to estimate the pairwise distance between networks, yielding $\hat{\mathcal{D}}$. Applying MDS to $\hat{\mathcal{D}}$ yields the mirror estimate $\{\hat{\psi}(t)\}$. To further simplify the change point detection problem, we apply the manifold learning method ISOMAP [7] to $\{\hat{\psi}(t)\}$, yielding the *iso-mirror*, and perform subsequent inference using the iso-mirror representation. For convenience, the ISOMAP representation will also be denoted as $\{\hat{\psi}(t)\}$.

5 Results

5.1 Time series of organoid networks data

Our time series of organoid networks consists of 40 time stamps $\{1, 2, \dots, 40\}$; each time stamp corresponds an effective connectivity graph G_t with adjacency matrix A_t . Each graph is directed, weighted, and hollow. All graphs have the same vertex set $V = \{1, 2, \dots, n\}$ with $n = |V| = 124$, although some of the graphs contain isolated vertices. See Figure 1.

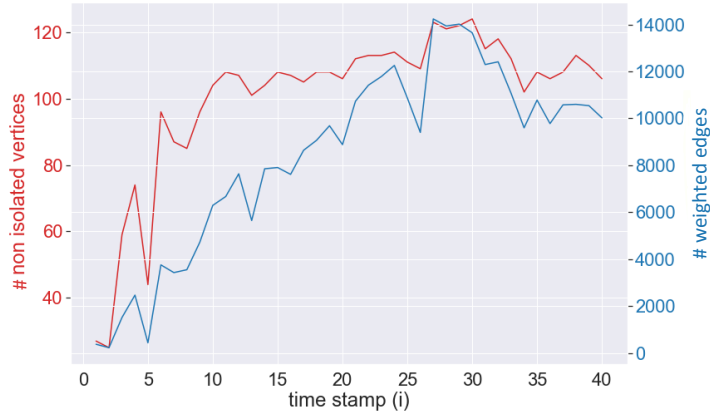


Figure 1: The number of non-isolated vertices and the number of edges for the graphs at each of the 40 time stamps.

5.2 Putative 1-1 correspondence

For this time series of organoid networks, inferred neuron location gives a putative 1-1 vertex correspondence across the graphs. We assess this correspondence via graph matching using the objective function value (OFV) $f(A, B; P)$. The OFV for the putative 1-1 correspondence is given by $f(A, B; I)$ where I is the identity matrix. We denote the FAQ output for matching adjacency matrices A and B initialized at C as $P_{A,B;C}$. Typically we choose the barycenter $b = \frac{11^T}{n}$ as the initial point. For all times $i \in \{1, 2, \dots, 39\}$, we consider A_i, A_{i+1} and FAQ yields $P_{A_i, A_{i+1}; b}$ (denoted $P_{i, i+1; b}$ for short). In Figure 2 we compare $f(I) = f(A_i, A_{i+1}; I)$ and $f(P_{i, i+1; b}) = f(A_i, A_{i+1}; P_{i, i+1; b})$. Although $f(P_{i, i+1; b})$ is always larger than $f(I)$, the two OFVs are close to each other for all time stamps, indicating that the putative 1-1 correspondence is close to FAQ's solution.

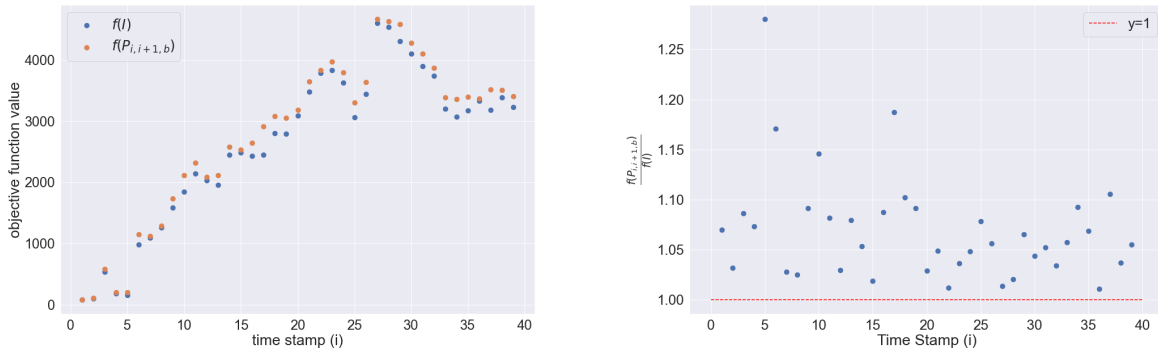


Figure 2: Comparison of OFV using I and $P_{i, i+1; b}$ for 39 pairs of graphs, demonstrating that FAQ increases the OFV only slightly. Left: $f(I)$ and $f(P_{i, i+1; b})$. Right: $\frac{f(P_{i, i+1; b})}{f(I)}$.

To further assess the putative 1-1 correspondence, we consider a specific pair of adjacency matrices: A_{28}, A_{29} . We uniformly generate 100,000 random permutation matrices R and evaluate $f(R) = f(A_{28}, A_{29}; R)$. We plot the histogram in Figure 3. We also indicate $f(A_{28}, A_{29}; I)$, $f(A_{28}, A_{29}; P_{28, 29; I})$, $f(A_{28}, A_{29}; P_{28, 29; b})$ and $f(A_{28}, A_{29}; P_{28, 29; R})$, where R are 100 randomly drawn permutation matrices. We see that the putative 1-1

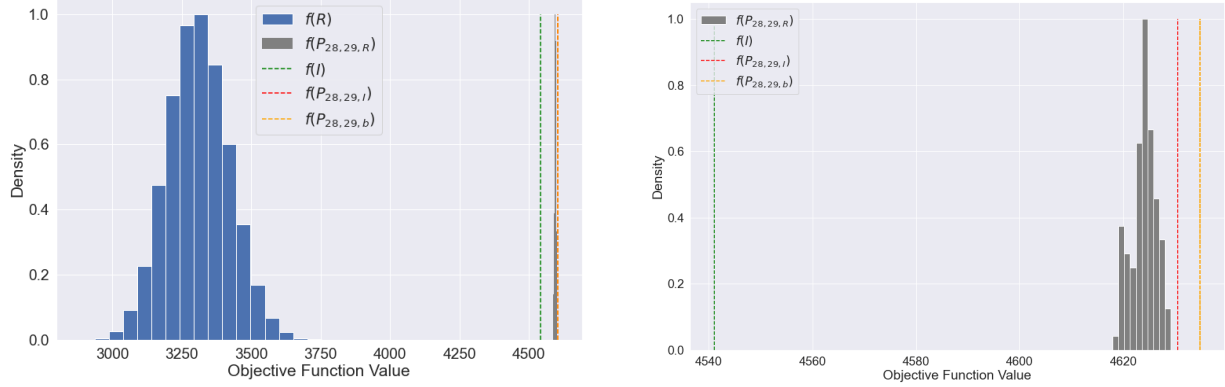


Figure 3: Matching A_{28} and A_{29} . Comparison of OFV for using $I, R, P_{28,29;b}, P_{28,29;I}$ and $P_{28,29;R}$. Left: Histogram demonstrating that OFV for R is not nearly as good as for the others. Right: Enlargement of the far right portion of the left figure, demonstrating that FAQ output at different initial points I, b and R improves the OFV only slightly compared to the putative 1-1, I .

correspondence performs better than all 100,000 instantiations of $f(R)$ and is close to $P_{28,29;b}, P_{28,29;I}$ and $P_{28,29;R}$. Thus we conclude that the putative 1-1 correspondence is sufficiently accurate, and we will proceed apace for mirror estimation and change point detection.

5.3 Change point detection

For the 40 graphs, time stamps are from 1 to 244, in days. We choose time stamps in $[150,230]$ to avoid growth and death regimes and keep 10 graphs. For these 10 graphs, we find the largest common connected component, which contains 112 vertices. The average number of edges for the largest common connected component is approximately 6130. We symmetrize the directed graphs, and use ranks in place of the raw edge weights. We use the putative 1-1 vertex correspondence across time. We apply our mirror estimation method to this time series of networks, and ISOMAP manifold learning yields the 1-dimensional representation of the dynamics $\{\hat{\psi}_t\}$ shown in Figure 4. As we see, the representation is approximately piecewise linear with an evident change of slope at $t = 4$, day 188.

Assuming the true underlying 1-dimensional representation $\psi(t), t \in [0, T]$, is piecewise linear and continuous, it is natural to define the change point t^* as the point when the slope changes. If we assume there is only one change point, then we can write

$$\psi(t) = \beta_0 + \beta_1 t + \beta(t - t^*)I(t > t^*).$$

Both the change point detection algorithm from [3] and the break point estimation for piecewise linear models from [4] yield an estimated change point $\hat{t}^* = 4$, day 188, which coincides with developmental changes as described in [9].

6 Conclusion

Reconstruction of effective connectivity networks of electrophysiologically active brain organoids reflect their structural (increasing number of neurons (nodes) and connections (edges)) and electrical development over time, as previously demonstrated in [9].

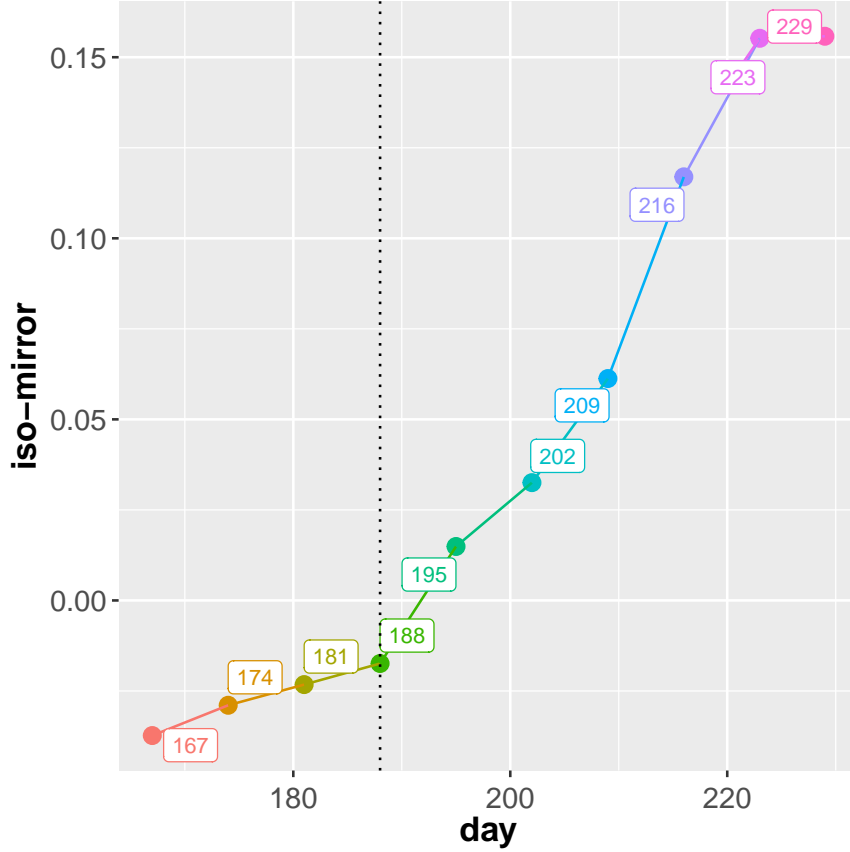


Figure 4: Discovering a change point in time series of inferred effective connectivity organoid networks via the iso-mirror. The x-axis is time stamp, in days. The y-axis is the ISOMAP representation of the estimated mirror $\{\hat{\psi}_t\}$. This indicates a change in the network dynamics at day 188.

By applying the spectral mirror estimation method to the time series of organoid networks, we obtain a 1-dimensional iso-mirror representation of dynamic inferred effective connectivity organoid networks. Two change point detection algorithms successfully detect the neuroscientifically significant change at day 188. At 188 days (~6 months), cortical organoids start showing inhibitory neurons and the percentage of astrocytes increases from 5% to 30-40% [9]. The resulting added complexity in the activity and network distribution of brain organoids is clearly detected by our algorithm.

Future work includes addressing two major theoretical issues of note, to make the change point inference formally principled. First, the theory in [2] requires a known 1-1 vertex correspondence across time. It remains to study the effect of errors in this correspondence, such as those inherent in our putative 1-1 correspondence deemed sufficiently accurate for practical purposes. In addition, it remains to study the entry-wise behavior of the error term $\epsilon(t) = \hat{\psi}(t) - \psi(t)$. For example: in [3] the proof of consistency of the change point estimator requires the error process to be stationary; in [4] the $\epsilon(t)$ are assumed to be i.i.d. normal to construct a confidence interval for \hat{t}^* . For now, [2] has shown that $\hat{\psi}(t)$ converges to $\psi(t)$ in Frobenius norm, that is $\sum_{t=1}^T (\epsilon(t))^2 \rightarrow 0$ with high probability, which is insufficient to conclude normality or stationarity.

References and Notes

- [1] Avanti Athreya, Donniell E Fishkind, Minh Tang, Carey E Priebe, Youngser Park, Joshua T Vogelstein, Keith Levin, Vince Lyzinski, Yichen Qin, and Daniel L Sussman. Statistical Inference on Random Dot Product Graphs: a Survey. *J. Mach. Learn. Res.*, 18(226):1–92, 2018. URL <http://jmlr.org/papers/v18/17-448.html>. 3
- [2] Avanti Athreya, Zachary Lubberts, Youngser Park, and Carey E Priebe. Discovering underlying dynamics in time series of networks. *arXiv preprint arXiv:2205.06877*, 2022. 1, 3, 6
- [3] Axel Bücher, Holger Dette, and Florian Heinrichs. Are deviations in a gradually varying mean relevant? a testing approach based on sup-norm estimators. *The Annals of Statistics*, 49(6):3583–3617, 2021. 1, 5, 6
- [4] Vito MR Muggeo. Interval estimation for the breakpoint in segmented regression: A smoothed score-based approach. *Australian & New Zealand Journal of Statistics*, 59(3):311–322, 2017. 1, 5, 6
- [5] Keiko Mugaruma, Ayaka Nishiyama, Hideshi Kawakami, Kouichi Hashimoto, and Yoshiki Sasai. Self-organization of polarized cerebellar tissue in 3d culture of human pluripotent stem cells. *Cell reports*, 10(4):537–550, 2015. 2
- [6] Francesca Puppo, Deborah Pré, Anne G Bang, and Gabriel A Silva. Super-selective reconstruction of causal and direct connectivity with application to in vitro ipsc neuronal networks. *Frontiers in Neuroscience*, 15:647877, 2021. 1, 2
- [7] Joshua B Tenenbaum, Vin de Silva, and John C Langford. A global geometric framework for nonlinear dimensionality reduction. *Science*, 290(5500):2319–2323, 2000. 3
- [8] Warren S Torgerson. Multidimensional scaling: I. theory and method. *Psychometrika*, 17(4):401–419, 1952. 3
- [9] Cleber A Trujillo, Richard Gao, Priscilla D Negraes, Jing Gu, Justin Buchanan, Sebastian Preissl, Allen Wang, Wei Wu, Gabriel G Haddad, Isaac A Chaim, et al. Complex oscillatory waves emerging from cortical organoids model early human brain network development. *Cell stem cell*, 25(4):558–569, 2019. 1, 5, 6
- [10] Joshua T Vogelstein, John M Conroy, Vince Lyzinski, Louis J Podrazik, Steven G Kratzer, Eric T Harley, Donniell E Fishkind, R Jacob Vogelstein, and Carey E Priebe. Fast approximate quadratic programming for graph matching. *PLoS One*, 10(4):e0121002, April 2015. URL <http://dx.doi.org/10.1371/journal.pone.0121002>. 1, 2